Synthesis and photophysical evaluations of fluorescent quaternary bipyridyl-1,8-naphthalimide conjugates as nucleic acid targeting agents

Gary J. Ryan,[a] *Robert B. P. Elmes*[a] *Susan J. Quinn*[a,b]* *and Thorfinnur Gunnlaugsson*[a]*

a) School of Chemistry and Centre for Chemical Synthesis and Chemical Biology, Trinity College, Dublin 2, Ireland. b) School of Chemistry and Chemical Biology, Centre for Chemical Synthesis and Chemical Biology, University College Dublin, Dublin 4, Ireland.

susan.quinn@ucd.ie, gunnlaut@tcd.ie

Abstract: A family of organic molecules containing the DNA intercalating chromophores, 4-nitro- and 4-amino 1,8-naphthalamide, conjugated to a diquat derivative by an 'orthogonal' phenyl spacer have been prepared, and characterized. Their binding interactions with double-stranded DNA was studied by a variety of spectroscopic techniques. These charged organic compounds are found to exhibit excellent binding affinities to DNA with binding constants comparable to those exhibited by metal complexes.

Keywords: DNA probes, naphthalimide, fluorescence, sensors, supramolecular systems

INTRODUICTION

The rational design and synthesis of molecules capable of binding DNA is a constantly evolving area of active research which is driven by the need for new treatments of diseases such as cancer, itself caused by malfunction of DNA.[1,2] In particular, molecules that exhibit multiple interactions through intercalation, groove binding and external electrostatic binding may allow for both stronger binding, increased selectivity and greater specificity.[3-11] Such systems have been the focus of our research for a number of years now.[10,12] The excellent binding properties of polypyridyl transition metal ion complexes, such of Ru(II), Os(II), Rh(III) and Cr(III) have led to interest in the use of metal complexes as anchors to locate a secondary external binding group or facilitate an electrostatic interaction.[13,14] Indeed we have used such complexes to prepare a range of new DNA binders. An example of our design is the formation of several 'rigid' ruthenium tris bipyridyl naphthalimide complexes that exhibit strong DNA binding, and photoinduced DNA cleavage upon irradiation.[15] We have also developed mixed *f–d* metal ion complexes, the emission of which is modulated upon binding DNA, both in the visible and NIR regions of the spectrum.[15] Furthermore, in related research we have also prepared purely cationic organic naphthalimide cleft-like molecules that provide shape recognition as DNA binders.[16]

The intercalative properties of extended polypyridyl ligands such as dppz (dipyrido[3,2-a:2',3'-c]phenazine) have been extensively exploited for DNA binding particularly in Ru(II) and Rh(III) polypyridyl complexes.[17-24] In a further development, Thomas *et al*., have recently developed quaternarized dppz molecules and their derivatives, as DNA binders, and shown these exhibit excellent binding affinity.[25] In this work the binding of the extended form of the dppz ligand, dqdppn, to a deformity in the double helix was noted. Inspired by this work, we have recently developed the synthesis and evaluated the binding of related dppz-functionalized structures to DNA.[26] We[14,15] and others,[27] have also shown that the naphthalimide structure can function as a strong DNA binders. Based on this work, and our general interest in the use of 1,8-naphthalimide based structures as probes and sensors,[28] we set out to develop new 1,8-naphthalimide based ligands capable of participating in both

DNA intercalative mode of action and groove binding. Our systems comprise a cationic bipyridine moiety conjugated to either a 4-nitro- or a 4-amino-1,8-naphthalimide *via* a phenyl spacer, at the *meta* or the *para* positions, yielding **1-3**, Figure 1. These bi-functional structures should bind strongly to DNA through synergetic action, where the quaternarized bipyridine (diquat) moiety is expected to result in strong electrostatic binding to the phosphate backbone of DNA, and hence a groove binding, while the naphthalimide moiety may participate in DNA intercalation, or possible groove binding. The relationship between the two DNA binding motifs caused by the non-conjugated phenyl spacer can be described as being linear, *e.g.* **1** or wedged, *e.g.* **2-3** and would be expected to influence the binding in a unique manner, the result of which would be expected to modulate the photophysical properties of both moieties. Herein, the synthesis of **1-4**, their ability to bind to DNA and various homopolymers are described. To the best of our knowledge, these are the first examples of the use of the 1,8-naphthalimide units in this manner, but these strongly visibly absorbing fluorophores (in the case of the 4-amino-1,8-naphthalimides λ_{max} ~ 450 nm) and long wavelength emitting fluorophores, make them highly attractive for use as biologically, and in particularly DNA, targeting agents.[29]

RESULTS AND DISCUSSION

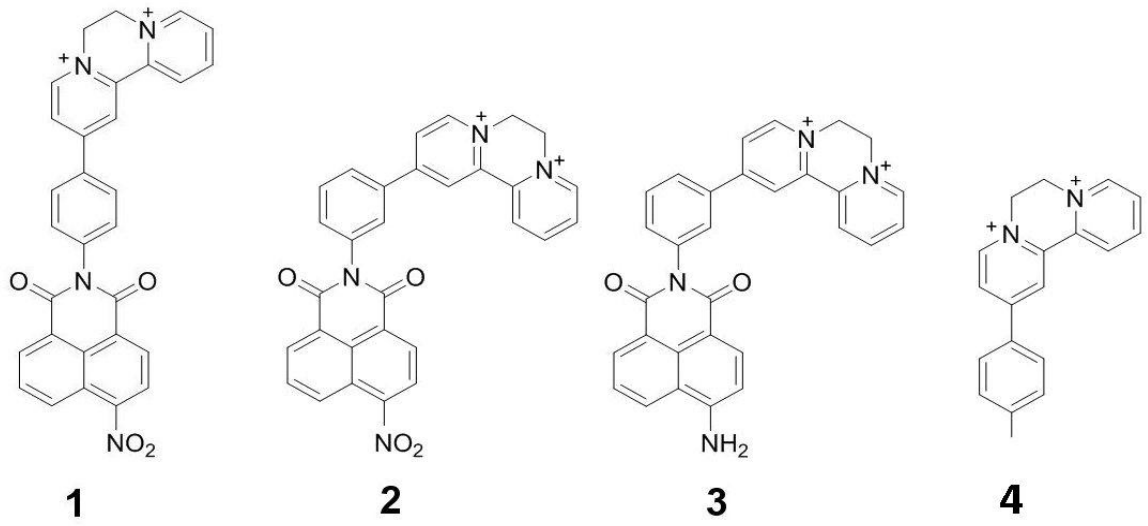

Figure 1. Family of quaternary bipyridine conjugated naphthalimides **1-3** studied herein and the reference compound **4**, all formed as their Cl^- salts.

Synthesis of compounds 1-4: The title compounds **1-3** were synthesized as outlined in Scheme 1 (the synthesis of control diquat compound **4** is shown in Supporting Information). The synthesis of compound **5** has previously been reported by us.[16] The synthesis of the meta aniline functionalised bipyridine **10**, needed for the synthesis of **11**, was easily achieved by adapting a literature procedure previously reported for the synthesis of the *para* analogue.[30] This involved the synthesis of compound **7** (formed from **6**, which was synthesised from 3-nitrobenzaldehyde using established procedure) (1 eq.), 2-pyridacyl pyridinium iodide (1 eq.) and ammonium acetate (8 eq.) were added to H_2O and the mixture heated at reflux for 5 hours. The solid was filtered, and washed with water and acetone to give the ammonium salt of the 4-(nitrophenyl)-6-carboxylate-2,2'-bipyridine, **8**. This compound was not purified any further, and immediately heated under vacuum until evolution of CO_2 ceased. The resulting black solid was dissolved in EtOAc (150 ml), activated charcoal added and the mixture refluxed for 15 min.

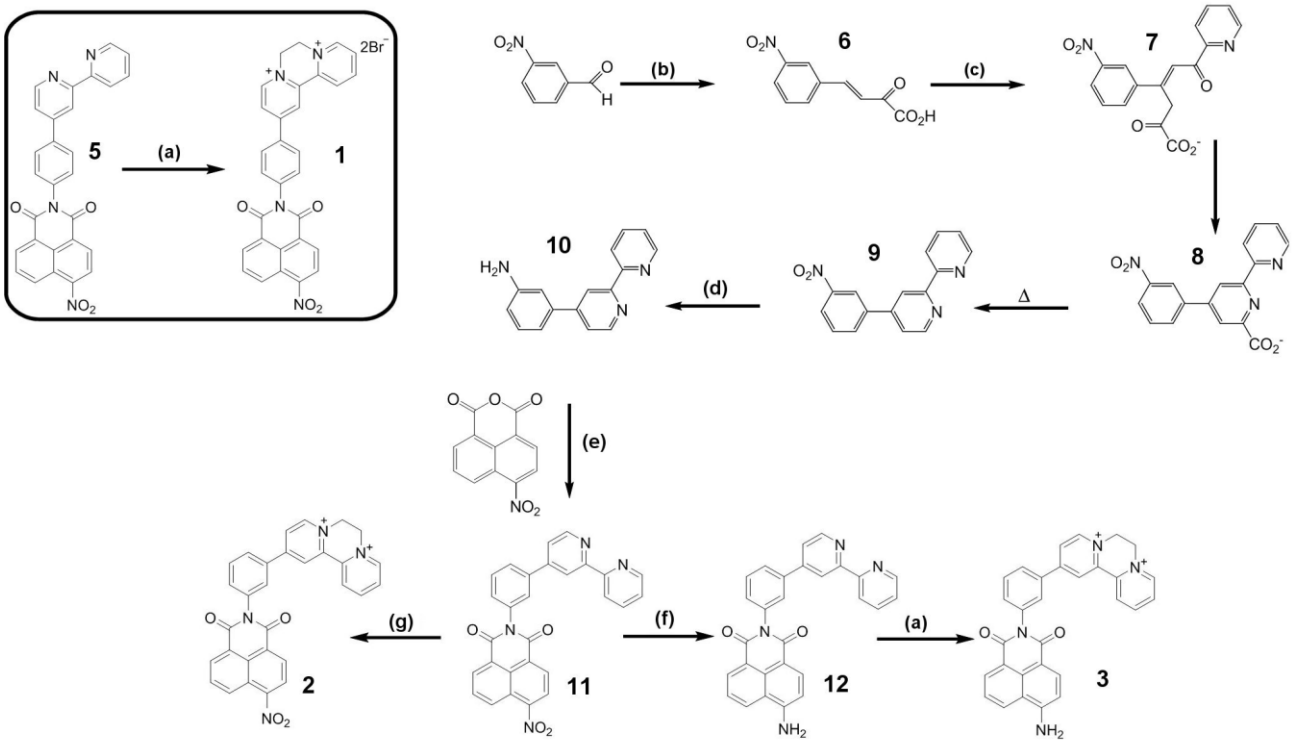

Scheme 1. Synthesis of 1,8-naphthalimide diquat compounds Reagents and conditions: (a) Excess dibromoethane, reflux 4.5 hrs, (b) $CH_3COCO_2^-$, EtOH, 2M NaOH, 2M HCl, (c) 2-pyridacyl pyridinium iodide, NH_4OAc, H_2O under reflux. (d) H_2NNH_2, Pd/C, EtOH, (e) EtOH, Argon atmosphere, 48 hrs, (f) H_2NNH_2, Pd/C, EtOH and (g) Excess dibromoethane reflux 48 hrs.

The mixture was filtered through a pad of celite and the solvent removed under reduced pressure, to give **9** as pale yellow solid in 37% yield. This product was reduced to the corresponding amino

derivative **10** using 10% Pd/C in EtOH, under reflux for one hour, followed by the addition of hydrazide monohydride, and further reflux for one hour. This gave the desired product as an off-white solid in 97% yield. This aniline derivative was reacted with 4-nitro-1,8-naphthalic anhydride in refluxing ethanol solution under inert atmosphere for 24 h giving **11** as a pale brown solid in 84 % yield. Reduction of **11** using hydrazine hydride and Pd/C in refluxing ethanol gave the 4-amino-1,8-naphthalimide product **12** as an orange solid in 94 % yield. The desired 4-nitro-1,8-naphthalimide structures **1** and **2** were formed by simply refluxing **5** and **11,** respectively, in dibromoethane for 48 hours, followed by isolation of the resulting precipitate by suction filtration. The collected solids were washed repeatedly with acetone and ether, to remove any unreacted starting material, giving **1** and **2** as a brown solid in high 80% yield as dibromide salts.

In contrast, the synthesis of **3** by this method was problematic and resulted in the formation of unidentified decomposition products. However, by reducing the reaction time to 4.5 h we were able to successfully obtain **3** as an orange solid, albeit in a much lower 1.6% yield. A number of methods were

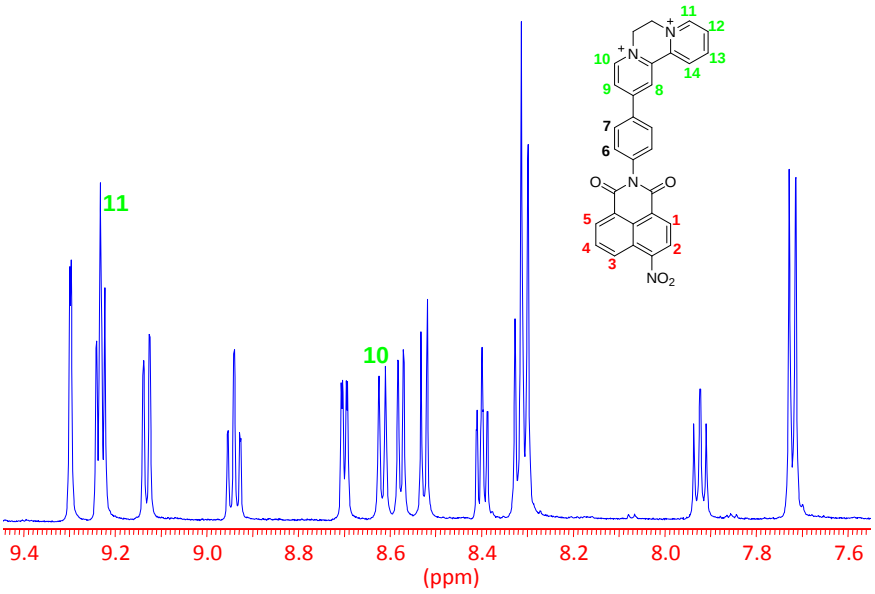

Figure 2. The ^{1}H NMR spectrum of **1** (D_2O, 400 MHz) showing the aromatic region.

subsequently explored with the view of improving the yield of the formation of **3**. These included reduction of the corresponding quarternarized nitro conjugate **2**, by hydrogenation, however, this did not

furnish the desired product. Also the condensation of **10** with 4-amino-1,8-naphthalic anhydride to afford an amino substituted ligand precursor **12** directly proved unfruitful. The bromide counter-ions for **1-3** were exchanged for chloride using Amberlite ion exchange resin (Cl- form). These products were fully characterized, see experimental. As an example Figure 2 shows the partial ^{1}H NMR for **1** clearly showing contributions from the naphthalimide as well as the diquat moiety. For comparison the ^{1}H NMR for **3** is shown in Figure S1 (Supporting Information). For comparison studies the control molecule **4** was formed in analogous manner from 4-(4-methylphenyl)-2,2'-bipyridne in 92 % yield (See Supporting Information).

Steady-state characterization: Having successfully synthesized **1-3**, their photophysical properties were characterized. The absorption spectrum of the linear derivative **1**, recorded in 10 mM phosphate buffered solution, is given in Figure 3. Three different absorption maxima are present, a sharp band at 282 nm, and two overlapping (but distinguishable) bands with λ_{max} at 320 and 338 nm, respectively. Comparison of this spectrum with those obtained for the water soluble controls, *N*-

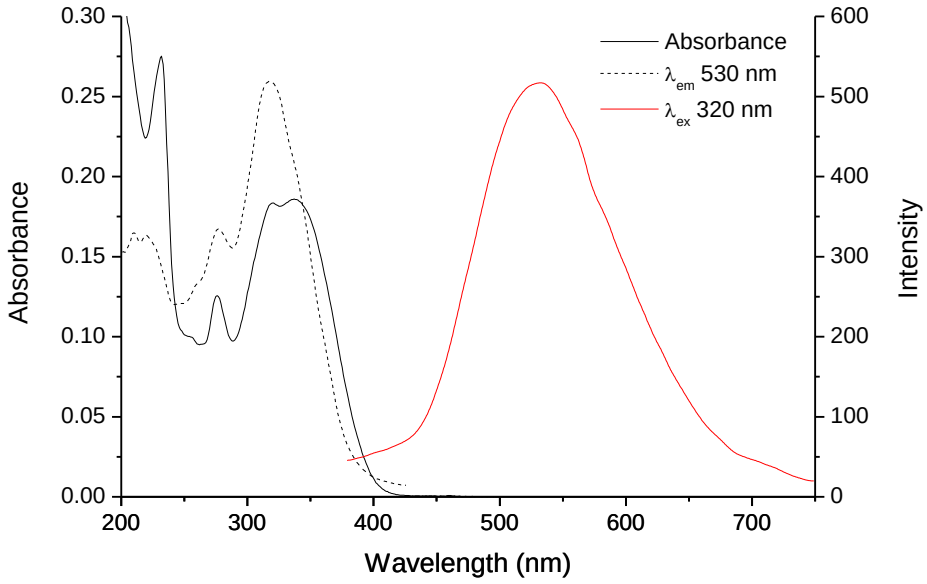

Figure 3. The UV/Visible absorption and the fluorescence excitation and the emission spectra of **1** (6.5 μM) when recorded in 10 mM phosphate buffer at pH 7.

(propylammonium)-4-nitro-1,8-naphthalimide **13**, and the diquat **4**, revealed some differences, (Figure S2 Supporting Information). The π-π* of 4-nitro-1,8-naphthalimide in **1** (338 nm) are found to be blue

shifted from that observed in **13** (354 nm). The diquat control **4** possesses a broad structured band at approximately 300 nm and second band at 350 nm. These bands are also found to be significantly shifted in **1**. The control spectra indicate the higher energy band at 320 nm in **1** to be diquat based, with the lower energy band (338 nm) composed of contributions from both the diquat and naphthalimide centres. This indicates a significant electronic interaction between the two components. In the case of the wedged structure **2** (Figure S3 Supporting Information) the naphthalimide band is further blue shifted from the position in **13** (See structure also in Figure S3). The absorption spectrum for amino compound **3** displayed bands at 434 nm and 311 nm (Figure S4 Supporting Information). An additive spectrum was also constructed for **3**, using the *N*-(propylammonium)-4-amino-1,8-naphthalimide control **14**,[16] (Figure S5 Supporting Information as well as the stricture). In this case the 1,3-phenyl conjugation was found to have very little effect on the 1,8-naphthalimide based absorption with a small red-shift for **3** (λ_{max} = 435 nm) compared to that of **14** (λ_{max} = 433 nm). Thus this band was assigned to the internal charge transfer (ICT) absorption character of the 4-amino-1,8-naphthalimide which arises due to the electron donating nature of the substituent.[28] However, other regions of the absorption spectrum were significantly different than that expected. In particular the band at 350 nm due to the diquat was found to essentially disappear with diminished absorption also observed at *ca.* 319 nm. This suggests that the conjugation has a significant effect on the absorption properties of the diquat moiety, which is to be expected given the strong electron accepting properties of diquat.[31]

The emission properties of **1** – **3** and the control compound **4** were next recorded. Excitation of **1** at λ_{max} gave a single emission band centered at 530 nm, as shown in Figure 3. This emission is not characteristic of a 4-nitro-1,8-naphthalimides, which typically exhibit weak fluorescence (*ca.* 450 nm due) to the electron withdrawing nitro group.[32,33] The excitation spectrum of **1** indicated the emission at 530 nm originated primarily from the diquat centre. Indeed, the excitation of **4** at 319 nm resulted in emission with two maxima, at 415 nm and 530 nm (Figure S6 Supporting Information). In light of this the emission in **1** was attributed to the diquat portion of the molecule. The absence of any emission from the nitro-1,8-naphthalimide in **1** may be indicative of a single excited state, arising from mixing of

energy levels of the constituent chromophores, or quenching of the 1,8-naphthalimide excited state by the attached diquat moiety. The related viologen moieties, covalently linked to 1,8-naphthalimides, have been shown to quench naphthalimide emission through intramolecular electron transfer.[28,34] In contrast the wedged system **2** displayed quite different, broad emission, upon excitation, more characteristic of the 4-nitro1,8-naphthalimide emission. This contribution of naphthalimide emission to this spectrum implies that the degree of interaction between the two chromophores in this system is less than in **1** with the wedged arrangement allowing for less effective overlap but also showing sensitivity of emission to the phenyl ring substitution. The excitation of the amino analogue **3** at 436 nm resulted in a single emission band centered at 550 nm. The band position is also characteristic of that previously observed for 4-amino-1,8-naphthalimides.[35] The excitation spectrum also showed the origin of emission to be from the naphthalimide centre. Excitation in the region of the diquat moiety at 311 nm also resulted in emission at 550 nm, though of reduced intensity, and was accompanied by an additional band *ca.* 370 nm. Thus the emission spectra indicate some mixing of the energy levels of the two components. This is quite different to that observed for the nitro analogue **2**, where little or no interaction was observed in the excited state. This is most likely a consequence of ICT dynamics which are sensitive to the conjugation at the imide position.

The redox behavior of the 4-nitro-1,8-naphthalimide-diquat conjugates **1** and **2**, provided further evidence of the interaction between the constituent chromophores resulting from the 1,3 arrangement of the phenyl spacer. Bridged bipyridine compounds such as diquat display well defined reduction and oxidation processes.[36] The 1,8-naphthalimides also display interesting electrochemistry depending on their nature and particular substitution pattern.[31,37] The cyclic voltammograms **1** and **2** were recorded in aqueous solution (Ag/AgCl in 100 mM phosphate buffer, at pH 7.0). Compound **1** possessed three reduction processes (Figure S7 Supporting Information); the peaks at – 0.28 V and – 0.78 V corresponding to sequential reduction processes at the diquat moiety,[36] while the peak at –0.49 V was attributed to the reduction of the 1,8-naphthalimide. The redox behavior of **2** was somewhat different, where two reduction processes were observed corresponding to reduction of the 1,8-naphthalimide and

the diquat moieties, respectively (Figure S8 Supporting Information). In this case, the second reduction of the diquat moiety was not observed. This we propose to be due to the smaller degree of interaction between the 1,8-naphthalimide and the diquat moiety, resulting from the wedged arrangement of this system, in contrast to the linear arrangement in **1** (which agrees with the results obtained from the steady state measurements above). The oxidation process for **2** occurs at a similar potential (–0.38 V) to that of **1,** as can be seen in Supporting Information. Importantly, in the case of **1** and **2**, the first two reduction potentials demonstrate the ease with which these structures can be reduced, which is a significant factor in their ability to lead to redox damage of the DNA polymer.

Investigation of DNA Binding with 1-4 Absorption Titrations: The binding of naphthalimides to DNA is typically accompanied by significant changes in the absorbance spectra[16,29] and is known to be influenced by the ring substituent.[38,39] The absorption spectra of molecules **1-4** were found to undergo significant change in the presence of increasing concentrations of DNA 10 mM phosphate buffer. In all cases (each titration was repeated several times, and were found to be fully reproducible) the addition of DNA resulted in hypochroism. For molecule **1** a 25 % hypochromic shift was observed (Figure S9 Supporting Information). A comparable change of 21% was observed for the wedged compound **2** (Figure S10 Supporting Information). However, more dramatic hypochromic changes were found for **3**, see Figure 4. Here, a 42 % decrease in the naphthalimide centered absorption band at 450 nm was observed, with an 11 % decrease found in the diquat centered band at 311 nm. Furthermore, the position of the 450 nm band was red-shifted shift by 11 nm at high concentrations of DNA. (Removed)

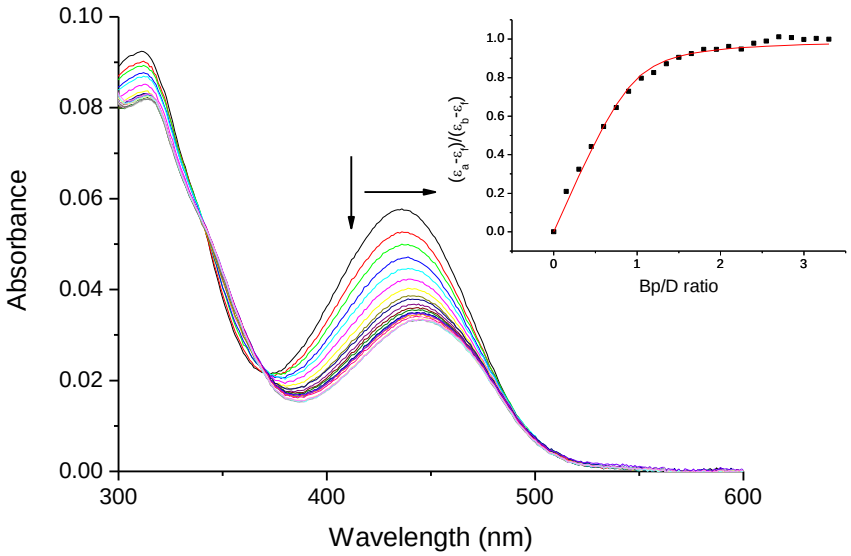

Figure 4. Changes in the UV/Visible spectrum of **3** (6.5 μM) upon addition of DNA (0 – 21.45 μM base pairs) in 10 mM phosphate buffer, at pH 7.

The changes in the absorbance spectra were analyzed using the Bard model.[39,40] In all three cases very strong binding was found, see Table 1, with binding constants in the range K = 1.7 × 10^7 (± 0.5) M^{-1} for **1** to 2.3 × 10^6 (± 0.5) M^{-1} for **3**. These binding constants compare very well with known DNA binders and are greater than those observed previously for naphthalamide based systems.[41] Indeed, the binding constant for **1** is comparable to that determined for the associated ruthenium polypyridyl complex [Ru(bpy)2(**5**)]Cl_2 which was found to bind to DNA with a binding constant of K = 4.5 × 10^6 (±0.7) M^{-1}.[12]

It is also interesting to note that the control diquat compound **4** was found to bind strongly to DNA, with a 32 % decrease in the absorption intensity at 355 nm (Figure S11 Supporting Information) and a binding constant of 2.8 × 10^6 (± 0.5) M^{-1}. The binding site size, for **1-3** are very similar *ca.* two base pairs, in contrast a binding site of five base pairs was determined for the control compound **4**. This clearly demonstrates the ability of compounds **1-3** to intercalate while compound **4** is expected to bind externally. This was confirmed by ionic strength studies. In the case of **4** the titration of concentrated salt solution resulted in complete reversal of binding at 30 mM NaCl (Figure S12 Supporting Information), while partial displacement was observed for **1-3** (Figure S13 Supporting Information).

Table 1. Various parameters obtained from the changes in the UV-Vis absorption spectra upon binding to DNA

No	Hypochroism	Bathochroism	Binding constant K (M^{-1})	Binding site size n (base pairs)	R^2
1	25 %	------	1.7×10^7 (± 0.5)	2.26 (± 0.04)	0.99
2	21 %	------	6.5×10^6 (± 1.8)	1.95 (± 0.06)	0.99
3	42 %	11 nm	2.3×10^6 (± 0.5)	1.98 (± 0.05)	0.99
4	32 %	8 nm	2.8×10^6 (± 0.5)	5.84 (± 0.21)	0.99

Fluorescence Emission Quenching Studies: All the molecules in the study were found to exhibit room temperature emission. Excitation of **1** at 336 nm results in emission centered at 530 nm, as discussed above. This emission is found to be quenched by 90 % in the presence of increasing concentrations of DNA, with a small blue shift being observed, see Figure 5. A similar behavior was observed for **4** (Figure S14 Supporting Information†) indicating that the changes observed for **1** are dominated by the interaction of the diquat moiety and DNA. The oxidizing nature of the diquat moiety

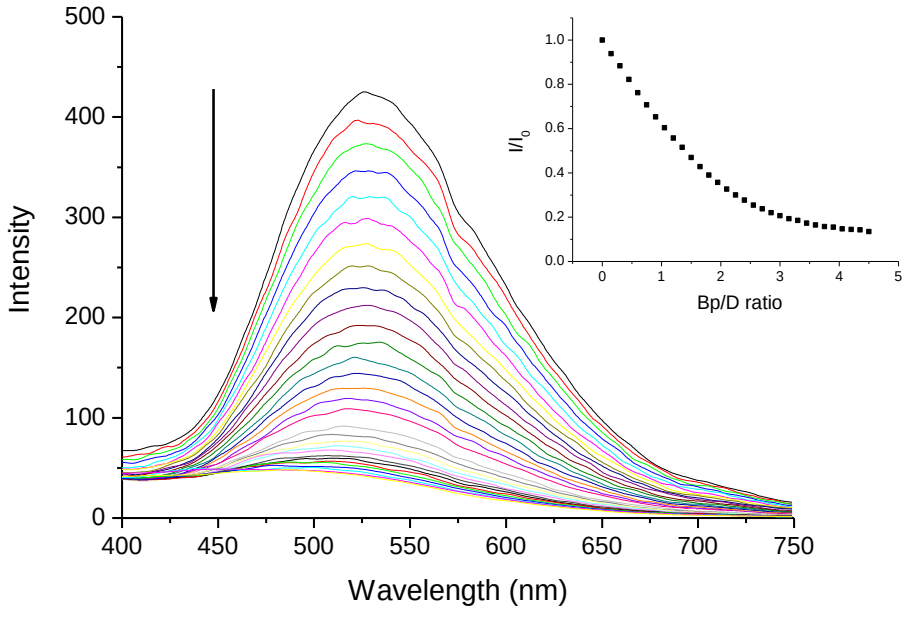

Figure 5. Changes in the emission spectrum of **1** (6.5 μM) (λ_{ex} 336 nm) upon addition of DNA (0 – 29.25 μM) in 10 mM phosphate buffer at pH 7.

strongly suggests that quenching of emission is due to electron transfer from the DNA bases to the diquat centre.[42] The efficiency of this process is improved when the oxidizing agent is held in close proximity to the bases. Hence the extent of quenching can be taken as a further indication of tight binding. In contrast to the significant changes seen in Figure 5, the wedged compound **2** exhibited much smaller changes in emission upon addition of DNA with 31% quenching observed (Figure S15 Supporting Information). (Removed)

Following on from this, the 4-amino compound **3** was considered. Titration with DNA resulted in significant quenching of the naphthalimide emission by 55 %, see Figure 6, again with only a very minor changes in the λ_{max}. The changes in the relative emission intensity for the λ_{max} were plotted against the base pair ratio (Bp/D) and are shown as insets in Figure 5 and 6 respectively. These plots clearly demonstrate similar binding behavior. However, we were unable to determine accurate binding constants from this data, regardless of the utilized models. Nevertheless the above results show the potential of our design for probing the binding interaction of such molecules with DNA. The difference in quenching behavior for **2** and **3** also arises due to steric effects of the ring substituent at the 4-position. (Removed) This illustrates, that in addition to the nature of the spacer, the nature of the ring

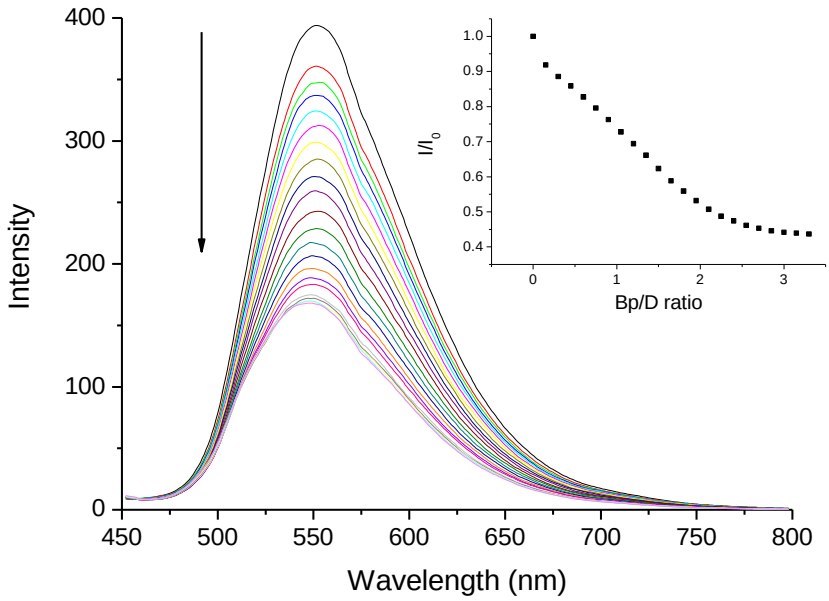

Figure 6. Changes in the emission spectrum of **3** (6.5 μM) (λ_{ex} 436 nm) upon addition of DNA (0 – 21.45 μM) in 10 mM phosphate buffer, at pH 7. buffer, at pH 7.

substituent on the naphthalimide greatly influence the binding and behavior of these molecules.

The interaction of **1** and **2** with DNA was evaluated by using ethidium bromide displacement assay and the binding constants were determined to be 1.7 x 10^7 M^{-1} and 2.4 x 10^7 M^{-1} respectively. (Removed) In the case of the ethidium bromide titration the binding constant for **1** is in agreement with that calculated from UV/Visible titration. However, the value for **2** is considerably removed from that determined by UV/Visible study, being almost an order of magnitude different. Compound **1** was determined to bind DNA with higher affinity, as the 1,8-naphthalimide may intercalate in a manner that is not restricted by the diquat, which point in the opposite direction, while binding of **2** to DNA might involve both intercalative interaction of the 1,8-naphthalimide, but also a considerable degree of groove association of the diquat part of the molecule, permitted by the wedged arrangement. In such a mode both parts of the molecule may effectively displace DNA bound ethidium bromide and thus the apparent affinity from the displacement assay is higher.

Studies of **1-4**, in the presence of different DNA alternating co-polymers were also carried out, with the aim of establishing if these compounds displayed any sequence selectivity in their binding. However, none of the systems displayed a marked preference in affinity for either $[poly(dA\text{-}dT)]_2$ or $[poly(dG\text{-}dC)]_2$. Furthermore, these compounds in general did not display any marked differences in their fluorescence spectra upon binding to AT or GC rich DNA. The titration profiles resulting from the addition of $[poly(dG\text{-}dC)]_2$ and $[poly(dA\text{-}dT)]_2$ to these compounds are shown in Figure S16 (Supportive Information).

Thermal Denaturation Studies: Having determined that **1-3** bind to DNA with significant changes in their spectroscopic properties we next evaluated these interactions using denaturation studies, as these can provide important information regarding the influence of binding on the stability of the DNA secondary structure. The presence of both nitro compounds **1** (linear) and **2** (wedged) were found to cause a dramatic change to the melting profile, with neither profile reaching a plateau at 90 ºC, see Figure 7. In these cases a T_m of greater than 75.0 ºC was assigned. The T_m value for DNA in the absence of the compounds was found to be 69 ºC. The reference **4** was also found to stabilize the double helix DNA, with T_m values of 73.4 and 75.4 ºC being obtained at a Bp/D ratio of 10 and 5, respectively. However, a very unusual melting profile was observed for **3** (Figure S17 Supporting Information). Between 30-60 ºC a decrease in absorbance was observed with an increase observed after 66 ºC. This negative melting curve structure has previously been associated with increasing DNA structure with increasing temperature, such as the formation of a duplex. It is possible that the presence of **3** results in disruption of regions of the duplex and these undergo change in the 30-60 ºC temperature range after

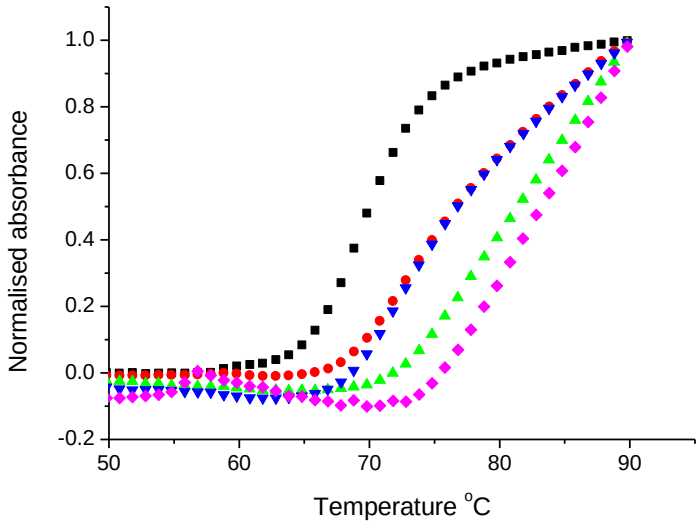

Figure 7. Thermal denaturation curves of DNA (150 μM) in 10 mM phosphate buffer, at pH 7, in the absence (■) and presence of **1** at a Bp/D ratio of 10 (●) and 5 (▲), and **2** at a Bp/D ratio of 10 (▼) and 5 (♦).

which the expected influence of bound **3** is observed.[44] These results are summarized in Table 2. Thermal denaturation studies on **1-3** were also carried out in the presence of $[poly(dA\text{-}dT)]_2$, which has a T_m of 47 ºC under buffered conditions. All three compounds were found to cause very large changes

in the observed T_m, see Figure 8a. While a 16.5 ºC difference in T_m was found for **1** even greater changes were found for the wedged compounds, which points to greater stabilization in the case of **2** (ΔT_m = 23 ºC). Furthermore, the melting profile of **2** revealed two regions of change, which was also

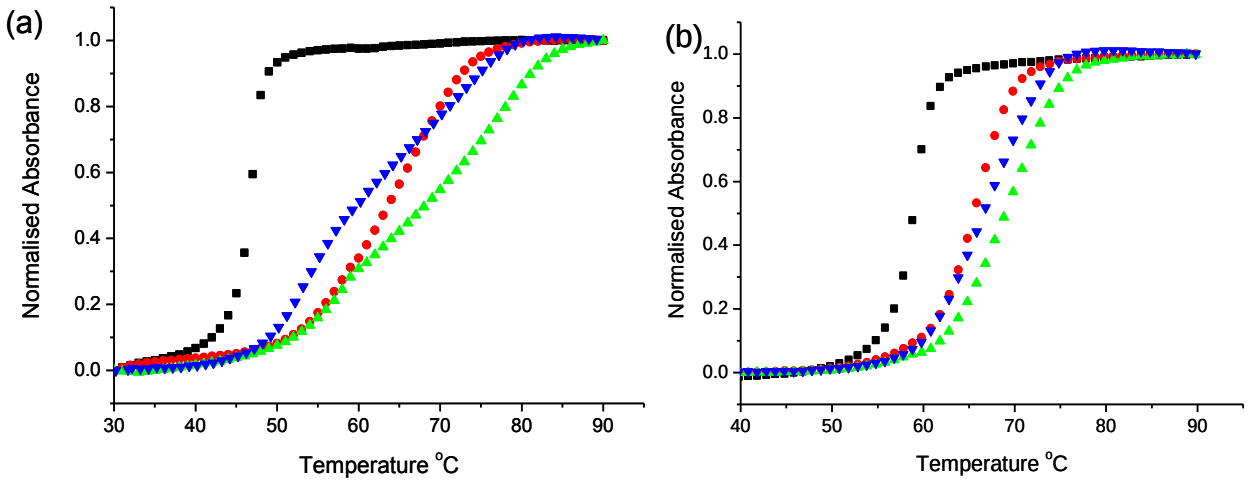

Figure 8. Thermal denaturation curves of $[poly(dA\text{-}dT)]_2$ (150 μM), in the absence (■) and presence of **1**(●), **2** (▲) and **3** (▼) all at a Bp/D ratio of 5. (a) 10 mM phosphate buffer, at pH 7 (b) 10 mM phosphate buffer + 50 mM NaCl, at pH 7.

observed for **3**.

The first order derivative of the data allowed these melting transitions to be readily distinguished (Figure S18 Supportive Information). Electrostatic interactions are expected to play an important role in any external binding for this reason measurements under conditions of increased ionic strength are desired. These were facilitated by the low temperature melting transition of $[poly(dA\text{-}dT)]_2$ which had 59 ºC in the presence of 50 mM NaCl (in 10 mM phosphate buffer). Significant changes in the melting profile were still observed for **1**-**3** probed under these conditions see Figure 8b. The greatest changes were again observed for the wedged nitro compound **2**, (ΔT_m = 10 ºC). In this case a single phase was observed in the melting profiles implying the loss of one of the binding modes. Thus the increased ionic strength is expected to have inhibited an electrostatic mode of interaction. The melting studies of **1** – **4**, illustrated the high affinity of all of the conjugate systems for DNA, with significant shifts in T_m values.

Table 2 Thermal denaturation data for compounds **1-4** (all reported with an error or ±0.5 ºC).

Sample Bp/D = 5	**Calf-Thymus Buffer** T_m/ ºC	**[poly(dA-dT)]$_2$ Buffer** ~T_m/ ºC	**[poly(dA-dT)]$_2$ Buffer + 50mM NaCl** ~T_m/ ºC
Absence	~69	47	59
1	> 75	64	66
2	> 75	70	70
3	~72	58	67
4	~75	-	-

Circular and Linear Dichroism (CD) Studies: To shed further light on the binding mode of these molecules their interactions with DNA were studied using both CD and LD. For the former, the titrations were carried out by varying the concentration of **1-4** in the presence of a constant concentration of DNA and considering the induced circular dichroism (ICD) signal, using normal experimental procedures. Such induced CD signals are a very useful tool for the determination of groove versus intercalative binding.[45-46] In the case of the linear nitro compound **1**, increasing concentration resulted in the appearance of a weak (~2.5 mdeg) positive induced CD signal at 352 nm

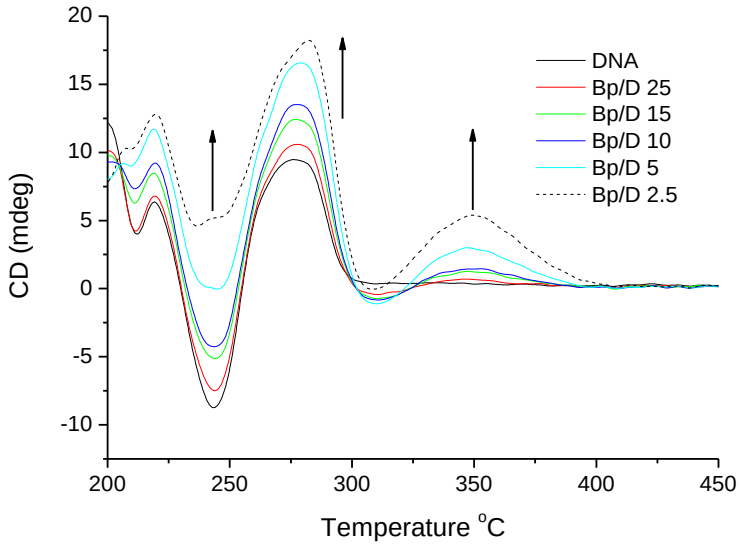

Figure. 9 Circular dichroism curves of DNA (150 μM) in 10 mM phosphate buffer, at pH 7, in the absence and presence of **2** at varying ratios.

(Figure S19). This signal was found to persist at higher salt concentrations (100 mM NaCl). The greatest changes were observed for the wedged compound **2**, see Figure. 9. A larger positive signal (~5 mdeg) was observed at 350 nm with greater changes also observed at lower wavenumbers. Again this signal persisted in the presence of 100 mM NaCl. While the assignment of a binding mode from changes in the CD spectrum is not definitive, generally small changes imply intercalation, whereas larger signals are indicative of groove binding and proximity to the chiral sugar residues. (REMOVED) The origin of the induced signal at 350 nm for both **1** and **2** could arise due to either the naphthalimide component or the diquat. However, the increase in magnitude may imply more favorable groove binding interaction of the diquat component in the case of **2**, as the intercalating naphthalimide center is preserved. Significantly, no induced CD signal was observed for the diquat control **4**, which has a strong absorbance in the region 300-350 nm, (Figure S20). This indicates that the presence of the naphthalimide is required to allow strong associative bonding of the diquat moiety with the groove.

Having previously studied the binding of **1-4** to homopolymers, the CD titrations of **1** and **2** with synthetic polymers $[poly(dA\text{-}dT)]_2$ and $[poly(dG\text{-}dC)]_2$ were also performed (Figure S21 Supporting Information). Large ICD was observed for both molecules in the presence of the polymers, particularly in the region above 300 nm, with ICD greater than that seen upon binding to DNA. The structure of the ICD band in the visible region was broader and more closely in agreement with the absorption spectrum of the compound. This suggests that structural differences in groove size in both homopolymers allows for additional interactions between the sugar environment and chromophores of **1** and **2**. Thus, while the strength of binding may not be very different between the homopolymers the nature of the binding interactions are somewhat modified.

Interestingly, in the case of **3** an additional induced CD band was observed to grow in at *ca.* 311 nm, and a less intense band at *ca.* 440 nm (Figure S22). Furthermore, in contrast to the signals observed for **1** and **2**, both ICD bands were negative. From the absorption spectrum (Figure S5) the band at 311 nm can be seen to originate from the diquat moiety while the band at 440 nm, is assigned to the 1,8-naphthalimide group. The relative intensities of these bands imply that the naphthalimide is intercalating and that the diquat is held close to the sugar groups with some partial intercalation of the linker group. The negative induced signals has previously been observed for intercalating naphthalimide bi-functionalized spermine compounds[44] and may arise due to the better intercalating nature of the amino substituted naphthalimide, as noted previously.[38]

To further investigate this we carried out LD-investigation where compounds **1** and **2** were studied in the presence of DNA. The changes in the LD spectrum for both, when recorded in 10 mM phosphate buffer solution with P/D ratio of 3, are shown in Figure 10. For the linear structure **1**, Figure 10a, it can be seen that both negative and positive signals are observed, this suggesting that contribution from both groove and intercalation mode of binding to DNA for **1**. These results support our finding above that both chromophores are contributing to the overall binding, though through different mode of

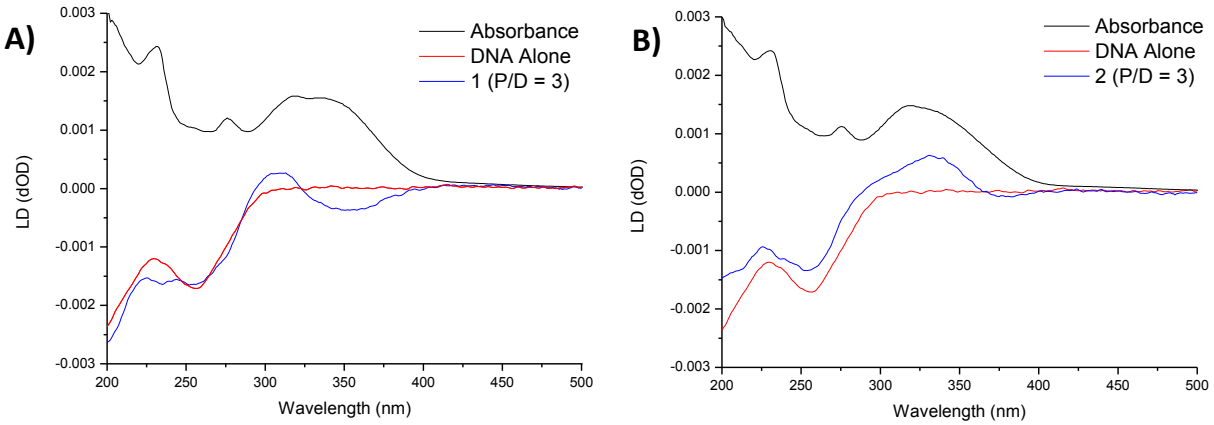

Figure. 10 Linear dichroism curves of DNA (150 μM) in 10 mM phosphate buffer, in the presence of **1** (a) and **2** (b) shown in blue. The LD-spectra of DNA (in red) and the UV-Vis absorption spectra of both **1** and **2** (in black) are included for reference.

interactions. Similarly, compound **2**, the wedged derivative also showed significant changes in the LD upon binding to DNA, where the contribution from groove binding seem to be increased in comparison

to compound **1**, suggesting that groove binding is the dominant mode of interaction, confirming the results seen in the CD spectra of **2** above.

Conclusion

In conclusion, we have demonstrated the high binding affinity of a family of new bipyridyl-derivatised naphthalimide molecules that exhibit binding affinities greater than that previously reported for naphthalimide systems and, in the case of **2**, comparable to that of the parent metal complex. The dramatic impact on the melting temperature and induced CD signals indicate that molecules such as **1** and **2** interact through intercalation, while LD measurements support stronger groove binding interactions in the case of **2**. This is further supported by the persistence of behavior under conditions of increased ionic strength. Denaturation experiments also reveal multiple modes of interaction including unusual phenomenon which may be due to changes in the secondary structure of DNA due to the cationic nature of the diquat molecule. The fluorescence titrations also reveal the different response of charge transfer sensitive and electron-mediated, quenching mechanisms to the DNA binding event. The binding is found to be sensitive to the ring substituent and the nature of connectivity. Overall the DNA titrations reveal that both the diquat and naphthalimide moieties contribute to the enhanced binding. These results clearly demonstrate how simple modification (in this case through quaternarization) of ligands designed to be employed in DNA binding metal complexes; can transform them into effective DNA binding ligands in their own right. These molecules are currently the focus of an in-depth biological study to evaluate their therapeutic potential this will be the subject of a future publication.

Experimental

Materials and Instrumentation: All NMR spectra were recorded using 400.13 MHz for ^{1}H NMR and 100.6 MHz for ^{13}C NMR, or a 600.1 MHz for ^{1}H NMR and 150.2 MHz for ^{13}C NMR. Shifts are referenced relative to the internal solvent signals. High resolution mass spectra were determined by a

peak matching method, using leucine Enkephalin, (Tyr-Gly-Gly-Phe-Leu), as the standard reference (m/z = 556.2771). The luminescence quantum yields were calculated by comparison with $[Ru(bpy)_3]^{2+}$. Circular dichroism (CD) spectra were recorded at a concentration corresponding to an optical density of approximately 1.0, in buffered solutions. All reagents and solvents were purchased commercially and used without further purification. Anhydrous solvents were prepared using standard procedures. Calf thymus and salmon testes DNA was used in this study, both of which have 33% G:C Solutions of DNA in 10mM phosphate buffer (pH 7) gave a ratio of UV absorbance at 260 and 280 nm of 1.86:1, indicating that the DNA was sufficiently free of protein. Its concentration was determined spectrophotometrically using the molar absortivity of 6600 M^{-1} cm^{-1} (260nm). Poly(dAdT)poly(dAdT) and poly(dGdC)poly(dGdC) concentrations determined spectrophotometrically using the molar absortivities of 6600 M^{-1} cm^{-1} (262nm) and 8400 M^{-1} cm^{-1} (254nm), respectively.

Synthesis

4-[*N*-(*p*-phenyl)-4-nitro-1,8-naphthalimide]-2,2'-ethylenebipyridyldiylium dichloride (1)*:* 4-[*N*-(p-phenyl)-4-nitro-1,8-napthalimide]-2,2'-bipyridine (0.33 g, 0.70 mmol, 1 eq.) was suspended into 30 ml of dibromoethane and heated under reflux for 48 hours. The reaction mixture was cooled to room temperature, the resulting precipitate collected by filtration and washed with acetone (5 ml) and hexane (5 ml). The product was dried under high vacuum. The product was dissolved in MeOH and stirred for 1 hour with Amberlite Ion exchange resin (Cl^-). The suspension was filtered and the solvent removed under reduced pressure giving the product as a brown solid (0.32 g, 80%). Calculated for $C_{30}H_{20}F_{12}N_4O_4P_2$: C, 45.59; H, 2.55; N, 7.09. Found: C, 45.37; H, 2.46; N, 6.88; Accurate MS (m/z) Calculated for $C_{30}H_{20}N_4O_4$ (M^{2+}): 500.1485. Found 500.1478; ^{1}H NMR δ_H (D_2O, 400 MHz): 9.23 (1H, s, Ar-H), 9.17 (2H, m, 2 x Ar-H), 9.06 (1H, d, *J* = 8.0 Hz, Ar-H), 8.87 (1H, m, Ar-H), 8.63 (1H, d, *J* = 6.0 Hz, Ar-H), 8.53 (1H, d, *J* = 9.0 Hz, Ar-H), 8.49 (1H, d, *J* = 7.5 Hz, Ar-H), 8.44 (1H, d, *J* = 8.0 Hz, Ar-H), 8.32 (1H, t, *J* = 7.0 Hz, Ar-H), 8.23 (3H, m, 3 x Ar-H), 7.83 (1H, t, *J* = 7.6 Hz, Ar-H), 7.65 (2H, d, *J* = 8.0 Hz, Ar-H), 5.30 (4H, d, *J* = 7.0 Hz, 2 x CH_2); ^{13}C NMR δ_C (D_2O, 100 MHz): 165.4, 164.4,

157.5, 149.8, 148.2, 147.1, 146.9, 139.6, 135.8, 134.8, 133.0, 132.7, 131.4, 130.7, 130.3, 130.0, 129.6, 128.6, 128.4, 128.2, 127.1, 125.7, 125.4, 124.3, 122.9, 121.5, 52.8, 51.7; IR ν_{max} (cm^{-1}): 1712 (m, -CO-N-CO-), 1523 (m, C-NO_2), 1347 (m, C-NO_2).

4-(3-Nitrophenyl)-2,2'-bipyridine (9): (*E*)-4-(3-Nitrophenyl)-2-oxo-3-butenoic acid (2.13 g, 9.64 mmol, 1 eq.), 2-pyridacyl pyridinium iodide (3.14 g, 9.64 mmol, 1 eq.), and ammonium acetate (5.95 g, 77.12 mmol, 8 eq.) were added to H_2O and the mixture heated at reflux for 5 hours. The solid was filtered, and washed with water (2 x 10 ml) and acetone (2 x 5 ml) to give the ammonium salt of the 4-(nitrophenyl)-6-carboxylate-2,2'-bipyridine. The ammonium salt was heated under vacuum with a heat gun until evolution of CO_2 ceased. The resulting black solid was dissolved in EtOAc (150 ml), activated charcoal added and the mixture refluxed for 15 min. The mixture was filtered through a pad of celite and the solvent removed under reduced pressure, giving the product as a pale yellow solid (0.92 g, 37%). m.p. 107 – 109 ºC; Accurate MS (m/z) Calculated for $C_{16}H_{12}N_3O_2$ (M+H): 278.0930. Found 278.0925; ^{1}H NMR δ_H ($CDCl_3$, 400 MHz): 8.78 (1H, d, *J* = 5.2 Hz, Ar-H), 8.71 (2H, m, 2 x Ar-H), 8.59 (1H, m, Ar-H), 8.47 (1H, d, *J* = 7.6 Hz, Ar-H), 8.29 (1H, dd, *J* = 1.2, 8.2 Hz, Ar-H), 7.86 (1H, dt, *J* = 1.8, 8.2 Hz, Ar-H), 7.68 (1H, t, *J* = 7.6 Hz, Ar-H), 7.56 (1H, dd, *J* = 1.7, 5.3 Hz, Ar-H), 7.36 (1H, m, Ar-H); ^{13}C NMR δ_C ($CDCl_3$, 100 MHz): 156.6, 155.1, 149.6, 148.8, 148.3, 146.3, 139.6, 136.6, 132.6, 129.7, 123.7, 121.6, 121.0, 120.9, 118.4; IR ν_{max} (cm^{-1}): 1525 (s, C-NO_2), 1343 (s, C-NO_2).

4-(3-Aminophenyl)-2,2'-bipyridine (10): 4-(3-Nitrophenyl)-2,2'-bipyridine (0.87 g, 3.14 mmol, 1 eq) and 10% Pd/C were added to EtOH (30 ml) and the mixture heated at reflux for 1 hour. Hydrazine monohydrate (98%) (2.01 g, 1.95 ml, 62.75 mmol, 20 eq.) was added and the mixture heated at reflux for 1 hour. The mixture was filtered through a pad of celite and the solid washed with CH_2Cl_2 (40 ml). The filtrate was washed with water, dried over $MgSO_4$, and the solvent removed under reduced pressure giving the product as an off white solid (0.75 g, 97%). m.p. 131 – 133 ºC; Accurate MS (m/z) Calculated for $C_{16}H_{14}N_3$ (M+H): 248.1188. Found 248.1193; ^{1}H NMR δ_H ($CDCl_3$, 400 MHz): 8.70 (1H, d, *J* = 3.5 Hz, Ar-H), 8.67 (1H, d, *J* = 15.1 Hz, Ar-H), 8.46 (1H, d, *J* = 8.0 Hz, Ar-H), 7.82 (1H, m,

Ar-H), 7.48 (1H, dd, *J* = 1.5, 5.0 Hz, Ar-H), 7.31 (1H, m, Ar-H), 7.25 (1H, m, Ar-H), 7.13 (1H, d, *J* = 7.5 Hz, Ar-H), 7.05 (1H, d, *J* = 2.0 Hz, Ar-H), 6.74 (1H, dd, *J* = 1.5, 8.0 Hz, Ar-H), 3.89 (2H, br s, NH_2); ^{13}C NMR δ_C ($CDCl_3$, 100 MHz): 156.0, 155.7, 149.1, 148.7, 146.7, 138.9, 136.5, 129.5, 123.4, 121.2, 120.8, 118.5, 116.9, 115.3, 113.1; IR ν_{max} (cm^{-1}): 3422 (w, -NH_2 stretch), 1626 (w, -NH_2 bending).

4-[*N*-(*m*-phenyl)-4-nitro-1,8-napthalimide]-2,2'-bipyridine (11): 4-(3-Aminophenyl)-2,2'-bipyridine 0.50 g, 2.04 mmol, 1 eq.) and 4-nitro-1,8-naphthalic anhydride (0.50 g, 2.04 mmol, 1 eq.) were suspended in HPLC grade ethanol and the mixture refluxed under an argon atmosphere for 48 hours. The reaction mixture was cooled to room temperature and ether added to further precipitate product, which was collected by suction filtration giving the product as a pale brown solid (0.81 g, 84%). Calculated for $C_{28}H_{16}N_4O_4.0.4H_2O$: C, 70.11; H, 3.53; N, 11.68. Found: C, 70.27; H, 3.35; N, 11.40; Accurate MS (m/z) Calculated for $C_{28}H_{17}N_4O_4$ (M+H): 473.1250. Found 473.1268; ^1H NMR δ_H ($CDCl_3$, 400 MHz): 8.81 (1H, s, Ar-H), 8.79 (1H, d, *J* = 4.5 Hz, Ar-H), 8.69 (4H, m, 4 x Ar-H), 8.62 (1H, d, *J* = 8.0 Hz, Ar-H), 8.46 (1H, d, *J* = 7.5 Hz, Ar-H), 8.17 (1H, m, Ar-H), 8.07 (1H, s, Ar-H), 8.04 (1H, d, *J* = 8.0 HZ, Ar-H), 7.98 (1H, dt, *J* = 1.5, 8.0 Hz, Ar-H), 7.86 (1H, m, Ar-H), 7.76 (1H, m, Ar-H), 7.59 (1H, d, *J* = 8.0 Hz, Ar-H), 7.49 (1H, m, Ar-H); ^{13}C NMR δ_C ($CDCl_3$, 100 MHz): 163.3, 162.5, 156.1, 155.0, 150.2, 149.3, 149.2, 147.2, 138.0, 137.4, 136.6, 131.7, 130.1, 130.0, 129.9, 129.6, 128.9, 128.8, 127.4, 127.3, 126.8, 124.4, 124.2, 123.4, 122.9, 121.4, 120.6, 117.4; IR ν_{max} (cm^{-1}): 1718 (w, -CO-N-CO-), 1524 (m, C-NO_2), 1350 (m, C-NO_2).

4-[*N*-(*m*-phenyl)-4-nitro-1,8-naphthalimide]-2,2'-ethylenebipyridyldiylium dichloride (2): Compound **11** (0.25 g, 0.53 mmol, 1 eq.) was suspended into 30 ml of dibromoethane and heated under reflux for 48 hours. The reaction mixture was cooled to room temperature, the resulting precipitate collected by filtration and washed with acetone (5 ml) and hexane (5 ml). The product was dried under high vacuum. The product was dissolved in MeOH and stirred for 1 hour with Amberlite Ion exchange resin (Cl^-). The suspension was filtered and the solvent removed under reduced pressure, giving the

product as a brown solid (0.25 g, 82%). Calculated for $C_{30}H_{20}F_{12}N_4O_4P_2$: C, 45.59; H, 2.55; N, 7.09. Found: C, 45.82; H, 2.42; N, 7.08; Accurate MS (m/z) Calculated for $C_{30}H_{19}N_4O_4$ (M^{2+}): 499.1406. Found 499.1411; ^{1}H NMR δ_H (D_2O, 400 MHz): 9.14 (1H, d, *J* = 6.0 Hz, Ar-H), 9.11 (1H, d, *J* = 6.5 Hz, Ar-H), 9.07 (1H, s, Ar-H), 8.95 (1H, d, *J* = 8.0 Hz, Ar-H), 8.79 (1H, t, *J* = 8.0 Hz, Ar-H), 8.54 (1H, d, *J* = 8.6 Hz, Ar-H), 8.46 (3H, m, 3 x Ar-H), 8.28 (1H, m, Ar-H), 8.23 (1H, d, *J* = 8.0 Hz, Ar-H), 8.11 (1H, d, *J* = 8.0 Hz, Ar-H), 8.02 (1H, s, Ar-H), 7.76 (2H, m, 2 x Ar-H), 7.62 (1H, d, *J* = 7.5 Hz, Ar-H), 5.26 (4H, d, *J* = 8.0 Hz, 2 x CH$_2$); ^{13}C NMR δ_C (D_2O, 100 MHz): 165.4, 164.4, 157.5, 149.7, 148.2, 147.1, 146.9, 139.6, 139.5, 135.8, 134.8, 133.0, 132.7, 131.4, 130.7, 130.3, 130.0, 129.5, 128.5, 128.4, 128.2, 127.1, 125.8, 125.7, 125.4, 122.9, 121.5, 52.5, 51.6; IR ν_{max} (cm^{-1}): 1715 (m, -CO-N-CO-), 1523 (m, C-NO_2), 1345 (m, C-NO_2).

4-[*N*-(m-phenyl)-4-amino-1,8-napthalimide]-2,2'-bipyridine (12): Compound **11** (0.30 g, 0.64 mmol, 1.eq.) was dissolved in DMF (30 ml) and MeOH (30 ml) added. To this was added 10% Pd/C (0.05 g) and the mixture heated at 65 ^{o}C for 1 hour. Hydrazine monohydrate (0.41 g, 0.40 ml, 12.74 mmol, 20 eq.) was added and the mixture heated at 65 ^{o}C for a further 16 hours. The reaction mixture was filtered through celite and the solvent removed under vacuum. The resulting residue was triturated with water to remove unreacted hydrazine and the solid isolated by filtration to give the product as an orange solid (0.27 g, 94%). Accurate MS (m/z) Calculated for $C_{28}H_{19}N_4O_2$ (M^{2+}): 443.1508. Found 443.1495; ^{1}H NMR δ_H (DMSO[D_6], 400 MHz) 8.78 (1H, d, *J* = 5.5 Hz, Ar-H), 8.69 (3H, m, Ar-H), 8.45 (2H, m, Ar-H), 8.23 (1H, d, *J* = 8.5 Hz, Ar-H), 8.00 – 7.92 (2H, m, Ar-H), 7.84 (1H, d, *J* = 5.0 Hz, Ar-H), 7.71 (2H, m, Ar-H), 7.53 – 7.47 (4H, m, Ar-H + NH2), 6.90 (1H, d, *J* = 8.5 Hz, Ar-H); ^{13}C NMR δ_C (DMSO[D_6], 100 MHz): 164.5, 163.6, 156.4, 155.4, 153.2, 150.5, 149.6, 147.8, 138.2, 138.0, 137.7, 134.3, 131.5, 130.7, 130.6, 130.1, 129.9, 128.1, 126.6, 124.7, 124.3, 122.7, 121.9, 121.0, 119.9, 117.9, 108.6, 108.2.

4-[*N*-(*m*-phenyl)-4-amino-1,8-napthalimide]-2,2'- ethylenebipyridyldiylium dichloride (3): 4-[*N*-(*m*-phenyl)-4-amino-1,8-napthalimide]-2,2'-bipyridine (0.15 g, 0.34 mmol, 1.eq.) was suspended in dibromoethane (30 ml) and the mixture heated at reflux for 4.5 hours. The reaction mixture was cooled

to room temperature, the resulting precipitate collected by filtration and washed with acetone (5 ml) and hexane (5 ml). The product was adsorbed onto a short pad of silica and purified using MeOH-NH_3(sat). A concentrated solution of NH_4PF_6 was added which gave a precipitate that could not be isolated by filtration. The product was extracted into DMF/CH_2Cl_2 and the solution concentrated under vacuum. The product was precipitated out by dropping into toluene and isolated by filtration. After drying under vacuum the product was obtained as an orange solid (0.003 g, 1.6%). Accurate MS (m/z) Calculated for $C_{30}H_{23}N_4O_2$ (M^{2+}): 471.1821. Found 471.1806; ^{1}H NMR δ_H (D_2O, 400 MHz): 9.11 (1H, d, *J* = 6.0 Hz, Ar-H), 9.00 (1H, d, *J* = 6.5, Ar-H), 8.93 (1H, s, Ar-H), 8.81 (1H, d, *J* = 8.5, Ar-H), 8.69 (1H, m, Ar-H), 8.35 (1H, d, *J* = 5.5 Hz, Ar-H), 8.23 (1H, m, Ar-H), 8.17 (1H, d, *J* = 8.0 Hz, Ar-H), 8.07 (1H, d, *J* = 8.0 Hz, Ar-H), 8.03 (1H, s, Ar-H), 7.96 (1H, d, *J* = 8.6 Hz, Ar-H), 7.90 (1H, d, *J* = 8.5 Hz, At-H), 7.58 (2H, m, Ar-H), 7.35 (1H, m, Ar-H), 6.54 (1H, d, *J* = 8.5 Hz, Ar-H), 5.21 (4H, m, $2CH_2$); ^{13}C NMR δ_C (D_20, 150 MHz): 166.3, 165.2, 157.3, 153.6, 148.1, 147.2, 146.8, 139.45, 139.38, 137.1, 135.0, 134.3, 133.2, 123.4, 131.2, 130.7, 130.2, 129.7, 128.8, 128.7, 128.2, 126.7, 125.0, 124.4, 120.0, 118.9, 109.4, 106.7, 52.5, 51.5.

4-(4-Methylphenyl)-2,2'-ethylenebipyridyldiylium dibromide (4): 4-(4-Methylphenyl)-2,2'-bipyridne (0.13 g, 0.53 mmol, 1.eq.) was suspended in dibromoethane (5 ml) and the mixture heated at reflux for 4 hours. The reaction mixture was cooled to room temperature, the resulting precipitate collected by filtration and washed with acetone (5 ml) and ether (5 ml). After drying under high vacuum the product was obtained as a yellow solid (0.21 g, 92%). Calculated for $C_{19}H_{18}Br_2N_2.1.25H_2O$: C, 49.81; H, 4.55; N, 6.11. Found: C, 49.94; H, 4.22; N, 6.07; Accurate MS (m/z) Calculated for $C_{19}H_{19}N_2$ (M^{2+}): 275.1548. Found 275.1555; ^{1}H NMR δ_H (D_2O, 400 MHz): 9.13 (1H, dd, *J* = 0.8, 6.0 Hz, Ar-H), 9.05 (1H, d, *J* = 2.3 Hz, Ar-H), 8.99 (1H, dd, *J* = 1.0, 8.2 Hz, Ar-H), 8.98 (1H, d, *J* = 6.52 Hz, Ar-H), 8.83 (1H, dt, *J* = 1.3, 8.0 Hz, Ar-H), 8.46 (1H, dd, *J* = 2.0, 6.5 Hz, Ar-H), 8.8 (1H, m, Ar-H), 7.91 (2H, d, *J* = 8.5 Hz, Ar-H), 7.22 (2H, d, *J* = 8.5 Hz, Ar-H), 5.25 (2H, m,

C$\underline{H}_2$), 5.18 (2H, m, C$\underline{H}_2$), 2.37 (3H, s, C$\underline{H}_3$); ^{13}C NMR δ_C (D_2O, 100 MHz): 159.0, 148.2, 147.0, 146.3, 145.0, 140.1, 139.3, 130.6, 130.5, 130.1, 128.4, 128.2, 126.2, 124.8, 52.7, 51.3, 20.7.

Absorption and Fuorescence Titrations: Solutions of calf-thymus DNA in 10mM phosphate buffer (pH 7) where found to give a ratio of UV absorbance at 260 and 280 nm of 1.86:1, indicating that the DNA was sufficiently free of protein. Titrations were performed by adding aliquots of stock DNA to the μM solutions of (1-4). All measurements were recorded at room temperature. The intrinsic binding constant K and the binding site size n were determined using the model derived by Bard *et. al.*[40]

Thermal Denaturation Experiments: Thermal denaturation experiments were performed on a thermoelectrically coupled Varian Cary 50 Spectrometer. The temperature in the cell was ramped from 20 to 90 ºC, at a rate of 1 ºC min^{-1} and the absorbance at 260 nm of DNA (150 μM) at 260 nm in 10 mM phosphate buffer at pH 7 in the absence and presence of 5-10 Bp/D ratio of (**1-4**), where Bp/D= base pairs to compound, was measured every 0.2 ºC.

Acknowledgements: We are grateful to Trinity College Dublin, Science Foundation Ireland, SFI and IRCSET (postgraduate studentship to G. J. Ryan) for financial support. We also wish to thank Dr. Michael E. G. Lyons and Dr. Gareth Keeley for assistance with the electrochemistry. We particularly would like to thank Prof. John M. Kelly for valuable discussions and his continuous support. This article is dedicated to his 65th birthday.

Supporting Information Available: General experimental description, synthesis and characterization of new compounds, various Figures and tables (see text for reference). This material is available free of charge via the Internet at http://pubs.acs.org.

REFERENCES

1. Neidle, S.; Waring, M. Eds. *Molecular Aspects of Anticancer Drug-DNA Interactions* CRC: Boca Raton, FL, 1993
2. Martínez, R. Chacón-García, L. *Curr., Med. Chem.,* 2005, **12**, 127.
3. Waring, M. J.; Chaires, J. B.; Armitage, B.A. *Top. Curr. Chem*. 2005, 253.
4. Kelly, J. M.; Tossi, A.; McConnell, D.; Oh Uigin, D. *Nucl. Acids Res.* 1985, **13**, 6017.
5. Jenkins, T. C. *Curr. Med. Chem.* 2000**, 7**, 99.
6. Dervan, P. B.; R. W. Burli, *Curr. Opin. Chem. Biol.* 1999**, 3**, 688.
7. Hannon, M. J. *Chem. Soc. Rev.* 2007, **36**, 280.
8. Erkkila, K. E.; Odom, D. T.; Barton, J. K. *Chem. Rev.* 1999**, 99**, 2777.
9. Schulman, L. S.; Bossmann, S. H.; Turro, N. J. *J. Phys. Chem.* 1995, **99**, 9283.
10. Vasudevan, S. Smith, J. A.; Wojdyla, M.; McCabe, T.; Fletcher, N. C.; Quinn, S. J. Kelly, J. M. *Dalton Trans.*, 2010, **39**, 3990.
11. Zeglis, B. M.; Pierre, V. C.; Barton J. K. *Chem. Commun*., **2007**, 4565.
12. Ryan, G. J.; Quinn, S.; Gunnlaugsson, T. *Inorg. Chem.*, **2008**, *47*, 401.
13. Lecomte, J.-P.; Kirsch-De Mesmaeker, A.; Demeunynck, M.; Lhomme, J. *J. Chem. Soc. Faraday Trans.* **1993**, *89*, 3261.
14. (a) Fu, P. K. L.; Bradley, P. M.; van Loyen, D.; Durr, H.; Bossmann, S. H.; Turro, C. *Inorg. Chem.* **2002**, *41*, 3808. (b) A. E. Friedman, J.-C. Chambron, J.-P. Sauvage, N. J. Turro, J. K. Barton, *J. Am. Chem. Soc.* **1990**, *112*,4960.
15. Nonat, A. M.; Quinn, S. J.; Gunnlaugsson, T. *Inorg. Chem.*, **2009**, *48***,** 4646.
16. a) Veale, E. B.; Gunnlaugsson, T. *J. Org. Chem*., **2010**, *75*, 5513. b) Veale, E. B.; Frimannsson, D. O.; Lawler, M.; Gunnlaugsson, T. *Org. Lett.*, **2009**, *11*, 4040.
17. Ortmans, Elias, B.; Kelly, J. M.; Moucheron, C.; Kirsch-DeMesmaeker, A *Dalton Trans.***,** **2004**, 668

18. Haq, Lincoln, P.; Suh, D.; Norden, B.; Chowdhry, B. Z.; Chaires, J. B. *J. Am. Chem. Soc.* **1995**,*117*, 4788.

19. Nair, R. B.; Teng, E. S.; Kirkland, S. L.; Murphy, C. J. *Inorg. Chem.* **1998**, *37*, 139.

20. Zeglis, B. M.; Valérie, C. P.; Kaiser, J. T.; Barton, J. K. *Biochemistry*, **2009**, *48*, 4247.

21. Gao, F.; Chao, H.; Zhou, F.; Yuan, Y.-X.; Peng, B.; Ji, L.-N. *J. Inorg. Biochem.* **2006**, *100*,1487.

22. Sun, Y.; Collins, S. N.; Joyce. L. E.; Turro, C. *Inorg. Chem.*, **2010**, *49*, 4257.

23. Gao, F.; Chen, X.; Wang, J.-Q.; Chen, Y.; Choa, H.; Ji, L.-N. *Inorg. Chem.*, **2009**, *48*, 5599.

24. Phillips, T.; Haq, I.; Meijer, A. J. H. M.; Adams, H.; Soutar, I.; Swanson, L.; Sykes, M. J.; Thomas, J. A. *Biochemistry.* **2004,** *43*, 13657.

25. (a) Waywell, P.; Thomas, J. A.; Williamson, M. P. *Org. Biomol. Chem.*, **2010**, *8*, 648. (b) Phillips, T.; Rajput, C.; Twyman, L.; Haq, I.; Thomas, J. A. *Chem. Comm.* **2005**, 4327.

26. Elmes, R. B. P.; Erby, M.; Cloonan, S. M.; Quinn, S. J.; Williams D. C.; Gunnlaugsson, T. *Chem. Commun*., **2011**, *47*, 686.

27. (a) Hariprakasha, H. K.; Kosakowska-Cholody, T.; Meyer, C.; Cholody, W. M.; Stinson, S. F.; Tarasova, N. I.; Michejda, C. J. *J. Med. Chem.* **2007**, *23*, 5557. (b) Cholody, W. M.; Kosakowska-Cholody, T.; Hollingshead, M. G.; Hariprakasha, H. K.; Michejda, C. J. *J. Med. Chem.* **2005**, *48*, 4474. (c) Brãna, M. F.; Ramos, A. *Curr. Med. Chem. Anti-Cancer* **2001**, *1*, 237. (d) Van Vliet, L. D.; Ellis, T.; Foley, P. J. Liu, L.; Pfeffer, F. M.; Russell, R. A.; Warrener, R. N.; Hollfelder, F.; Waring M. J *J. Med. Chem.* **2007**, *50*, 2326. (e) Brana, M. F., Cacho, M.; Garcia, M. A.; de Pascual-Teresa, B.; Ramos, A.; Dominguez, M. T.; Pozuelo, J. M.; Abradelo, C.; Rey-Stolle, M. F.; Yuste, M.; Banez-Coronel, M.; Lacal, J. C. *J. Med. Chem.* **2004,** *47*, 1391. (f) Aveline, B. M.; Matsugo, S.; Redmond, R. W. *J. Am. Chem. Soc.* **1997**, *119*, 11785. (g) Saito, I.; Takayama, M.; Kawanishi, S. *J. Am. Chem. Soc.* **1995**, *117*, 5590. (h) Fromherz, P.; Rieger, B. *J. Am. Chem. Soc.* **1986**, *108*, 5361.

28. (a) Duke, R. M.; Veale, E. B. Pfeffer, F. M.; Kruger P. E.; Gunnlaugsson, T. *Chem. Soc, Rev*., **2010**, *39*, 3936. (b) Veale, E. B.; Tocci, G. M.; Pfeffer, F. M.; Kruger, P. E.; Gunnlaugsson, T.

Org. Biomol. Chem. **2009**, *7*, 3447. (c) Veale, E. B.; Gunnlaugsson, T. *J. Org. Chem*. **2008**, *73*, 8073.

29. Johansson, O.; Borgstrom, M.; Lomoth, R.; Palmblad, J.; Hammarstrom, L.; Sun, L.; Akermark, B. *Inorg. Chem.* **2003**, *42*, 2908.
30. Coe, B. J.; Harris, J. A.; Brunschwig, B. S.; Garín, J.; Orduna, J. *J. Am. Chem. Soc.*, **2005**, *127*, 3284.
31. Kucheryavy, P.; Li, G.; Vyas, S.; Hadad, C.; Glusac K. D. *J. Phys. Chem. A*, **2009**, *113*, 6453.
32. Grabcheva, I.; Qianb, X.; Bojinovc, V.; Xiaob, Y.; Zhang, W. *Polymer* **2002**, *43*, 5731.
33. Le, T. P.; Rogers, J. E.; Kelly, L. A. *J. Phys. Chem. A.* **2000,** *104*, 6778.
34. (a) Parkesh, R.; Lee, T. C.; Gunnlaugsson, T. *Org. Biomol. Chem.* **2007,** *5*, 310. (b) Gunnlaugsson, T.; Lee, T. C.; Parkesh, R. *Org. Biomol. Chem*., **2003**, *1*, 3265. (c) Gunnlaugsson, T.; Glynn, M.; Tocci, G. M.; Kruger, P. E.; Pfeffer, F. M. *Coord. Chem. Rev*. **2006**, *250*, 3094. (d) Ali, H. D. P.; Kruger, P. E.; Gunnlaugsson, T. *New. J. Chem*. **2008**, *32*, 1153. (e) Duke, R. M.; Gunnlaugsson, T. *Tetrahedron Lett*. **2007**, *48*, 8043.
35. (a) Kucheryavy, P.; Li, G.; Vyas, S.; Hadad, C.; Glusac, K. D. *J. Phys. Chem. A* **2009**, *113*, 6453. (b) Saha, S.; Samanta, A. *J. Phys. Chem. A.* **2002**, *106*, 4763. (c) Braterman, P. S.; Song, J. I. *J. Org. Chem.* **1991,** *56*, 4678.
36. (a) Rogers, J. E.; Abraham, B.; Rostkowski, A.;; Kelly, L. A. *Photochem. Photobiol.* **2001**, *74*, 521. (b) Joseph, J.; Eldho, N.; Ramaiah, D. *Chem. Eur. J.* **2003**, *9*, 5926.
37. Stevenson, K. A.; Yen, S.-F.; Yang, N.-C.; Boykin, D. W.; Wilson W. D. *J. Med. Chem.* **1984**, *27*, 1677.
38. Wakelin, L. P. G.; Waring, M. J. *DNA Intercalating Agents. In Comprehensive Medicinal Chemistry*.; Pergamon: Oxford, 1990; Vol.
39. Carter, M. T.; Rodriguez, M. Bard, A. J. *J. Am. Chem. Soc.* **1989**, *111*, 8901.
40. (a) Rogers, J. E.; Weiss, S. J.; Kelly, L. A. *J. Am. Chem. Soc.* **2000**, *122*, 427. (b) Yen, S. F.; Gabbay, E. J.; Wilson, W. D. *Biochem.* **1982**, *21*, 2070.

41. Knapp, C.; Lecomte, J. P.; Kirsch-De Mesmaeker, A. Orellana, G. *J.l Photochem. Photob. B: Biology,* **1996**, *36*, 67.

42. Völker, J.; Makube, N.; Plum, G. E.; Klump, H. H.; Breslauer, K. J. *Proc. Nat. Acd. Sci* (USA) **2002**, *99*, 14700.

43. Tse, W. C.; Boger, D. L. *Acc. Chem. Res*., **2004**, *37*, 61.

44. MacMasters, S; Kelly L. A. *Photochem. Photobiol.* **2007**, *83*, 889.

45. Chen, Z.; Liang, X.; Zhang, H.; Xie, H.; Liu, J.; Xu, Y.; Zhu, W.; Wang, Y.; Wang, X.; Tan, S.; Kuang, S.; Qian X. *J. Med. Chem.*, **2010**, *53*, 2589.

46. Ott, I.; Xu,; Y.; Liu, J.; Kokoschka, M.; Harlos, M.; Sheldrick, W. S. Qian X. *Bioorg. Med. Chem.* **2008**, *16*, 7107.